Proceedings of the 9th International Conference on Civil Structural and Transportation Engineering (ICCSTE 2024)
Niagara Falls, Canada – June 13-15, 2024
Paper No. 112
DOI: 10.11159/iccste24.112

Neural predictional of Mechanical Properties of Fiber-Reinforced Lightweight Concrete Containing Metakaolin at High Temperatures

Hamidreza Moradi [1], Seyed Amir Hossein Hashemi [2]
[1]Department of Civil Engineering
Qazvin Branch, Islamic Azad University, Qazvin, Iran
hamidrezamoradi1360@qiau.ac.ir; hashemi@qiau.ac.ir
[2]Department of Civil Engineering
Qazvin Branch, Islamic Azad University, Qazvin, Iran
Niagara Falls.ca

Abstract - The fire hazard is a permanent threat to structures. Given the use of concrete in many structures, fire constitutes a considerable risk since it leads to a sudden collapse in these structures. If concrete made using Portland cement is subjected to heat, it experiences a number of transformations and reactions even in the case of a moderate temperature rise. Since aggregate occupies usually 65%-75% of concrete volume, the behavior of concrete at high temperatures is strongly dependent on the aggregate type. Therefore, the mix design of the fire-resistant concrete is of great importance. Obtaining a mix design capable of handling high temperatures requires the preparation of various concrete samples with different mix designs, which is both costly and time-consuming. Instead, simulating such tests in numerous iterations and performing the involved computations via simulation software results in cost savings and high accuracy. The present research used MATLAB modeling to obtain the compressive and tensile strengths of fiber-reinforced lightweight concrete containing metakaolin for various percentages of cement, gravel, sand, superplasticizer, and polypropylene fibers at high temperatures. The multilayer perceptron artificial neural network was employed for this purpose. The neural network was trained with 7 input layers, 2 output layers, and 1 hidden layer. As a result, it reached estimation accuracies of 99.06% and 97.16% for the training and testing data, respectively, and 99.05% for all the data, indicating the efficiency of the selected network.

***Keywords*:** Artificial neural network, high temperatures, lightweight concrete, polypropylene fibers, metakaolin

1. Introduction

It is expected that authors will submit carefully written and proofread material. Careful checking for spelling and grammatical errors should be performed. The number of pages of the paper should be from 4 to 8.

Papers should clearly describe the background of the subject, the authors work, including the methods used, results and concluding discussion on the importance of the work. Papers are to be prepared in English and SI units must be used. Technical terms should be explained unless they may be considered to be known to the conference community.

The materials constituting concrete possess low thermal expansion coefficients. This enables concrete to transfer heat very slowly and, as such, act as protection against heat. As a result, the appropriate selection of constituents can help make concrete fire-resistant. Aggregate composition is a significant factor in this regard. The use of special aggregates can improve the fire resistance and strength of concrete. Resistance to fire in concrete can be enhanced in various ways. Concrete made of Portland cement loses most of its properties when exposed to fire at temperatures higher than 300°C. Aggregates, which are commonly used in concrete, offer thermal stability up to a temperature of 300°C or 350°C. Moreover, concrete totally loses its structural function at temperatures higher than 600°C. The parameters controlling thermal performance are the aggregate type and free moisture in the concrete. The aggregate properties affecting concrete behavior at high temperatures include physical properties, such as thermal conductivity and thermal expansion, chemical properties, such as chemical stability at temperature, and thermal stability or integrity. At high temperatures, the hydrated cement in concrete is gradually dehydrated, and the concrete returns to water (vapor) and cement. This reduces the strength and the modulus of elasticity of the concrete. The use of natural and artificial lightweight aggregates in concrete preparation leads to cost-savings and in addition to weight reduction. This, in turn, results in a decrease in the dimensions of the load-bearing elements, the required amount of rebar, and transportation costs and an increase in fire resistance compared to normal concrete. Fiber-reinforced

concrete possesses such properties as excellent strength, high ductility, high energy absorption capacity, and cracking stability. Modern technology helps mankind to perform tasks faster, more accurately, and at a lower cost. The present paper aims to take a step in this direction by using artificial neural network (ANN) and experimental work. To this end, ANN and experimental results were used to predict the compressive and tensile strengths of fiber-reinforced concrete containing metakaolin (MK) at elevated temperatures.

Ayaz Ahmad et al. [1] compared the performance of supervised machine learning algorithms in predicting the compressive strength of concrete at high temperatures. They demonstrated that high temperatures reduce the strength of concrete. Meisam Bayat and Ali Delnavaz [2] predicted the lateral load capacity of steel shear walls (SSW) using ANN models with an accuracy of 96%. Using modeling in Abaqus, they modeled 144 different SSW samples with parameters such as plate thicknesses, stiffener thickness, diagonal stiffener distance, horizontal stiffener distance, and gravitational load as ANN inputs and determined the load-carrying capacity of the SWW as the ANN target. Muhammad Tufail et al. [3] investigated the effect of various coarse aggregates, namely limestone, quartzite, and granite, on the mechanical properties of the concrete subjected to high temperatures ranging from 95°C to 650°C. Granite concrete exhibited a higher compressive and tensile strength and modulus of elasticity at all test temperatures compared to quartzite and limestone concretes. Chi-Sun Poon et al. [4] conducted an experimental investigation on MK concrete at temperatures of up to 800°C. To this end, 8 normal and high-strength (HSC) concrete samples with 0, 5%, 10%, and 20% MK were prepared.The residual compressive strength, chloride ion penetration, porosity, and average pore size were measured and compared to those of other concrete mixes made of silica fume (SF), fly ash (FA), and ordinary Portland cement (OPC). According to the results, after an increase in compressive strength at 200°C, MK concrete experienced a larger drop in compressive strength and permeability-related durability compared to SF, FA, and OPC concretes. In the 400°C-800°C range, MK concrete suffered a large loss in compressive strength and had less residual strength compared to the other concretes. The effect of elevated temperature on the compressive strength of structural lightweight concrete (SLWC) containing various percentages of MK was examined by Bahar Demirel et al. [5]. Based on the results, the compressive strength increased with an increase in the amount of MK used in the SLWC. It was determined that the optimal MK/C ratio was about 18%. All the concrete samples exposed to high temperatures suffered strength loss. Nevertheless, the rate of strength loss decreased with an increase in the MK/C ratio. Hence, the MK/C ratios of the samples with minimum strength loss were optimal. Abid Nadeem et al. [6] investigated high-performance concrete (HPC) made of FA and MK at high temperatures and reported major strength and durability loss after 400°C for all mixtures. They concluded that a temperature of 400°C can be considered the critical temperature for a change in the properties of HPC. Sadegh Mehdipour et al. [7] demonstrated that a mixture of MK and steel fiber (SF) in concrete not only improves the mechanical properties and durability of rubberized concrete at elevated temperatures, but also introduces more environment-friendly mixtures compared to normal concrete by decreasing CO2 emission. Abdulrahman Albidah et al. [8] studied the behavior of MK-based geopolymer concrete at room temperature and temperatures above 200°C, 400°C, and 600°C. Their results indicated that, in all the mixtures, compressive strength decreased faster when the temperature exceeded 200°C. Nonetheless, the rate of decrease was lower when the temperature rose from 200°C to 400°C and from 400°C to 600°C. Olatokunbo M. Ofuyatan et al. [9] used the response surface method (RSM) and ANN to predict the mechanical properties of self-compacting concrete (SCC) with SF partially replacing cement and polyethylene terephthalate (PET) solid waste partially replacing sand. Their parity plots showed that neither ANN nor RSM exhibits prediction bias. However, ANN proved superior as a result of its higher accuracy and better suitability to the dataset. The present study mainly aims to examine the ANN approach to the accurate prediction of compressive and tensile strength in fiber-reinforced concrete containing MK at high temperatures. Apart from crystalline transformations occurring in aggregates during heating, a number of degradation reactions happen mainly in the cement paste, leading to gradual failure in the concrete structure. Sudden temperature rise results in significant changes in the chemical composition and microstructure of hardened Portland cement paste. These reactions are mostly in the form of dehydration reactions. Changes in the chemical composition and microstructure of hardened Portland cement paste occur gradually and continuously from room temperature up to 1000°C. With a rise in concrete temperature during the initial heating, considerable evaporation takes place from the larger pores near the concrete

surface. From 100°C onward, evaporation occurs faster, and water exits from the concrete near the surface due to the vapor pressure being higher than atmospheric pressure. At 120°C, the expulsion of water physically trapped in smaller pores or combined chemically begins and continues up to about 500°C, where the process is basically complete. From 30°C to 300°C, hydration of the hardened cement paste (first stage) happens along with evaporation, with the maximum hydration rate occurring at a temperature of 180°C. Portlandite decomposition ($Ca(OH)_2 \rightarrow CaO + H_2O$) takes place at 450°C-550°C [10]. At 570°C, $\alpha \rightarrow \beta$ quartz inversion occurs with an endothermic and reversible transformation. The hardened cement paste decomposes again between 600°C and 700°C, this time with the decomposition of the calcium-silicatehydrate phases and the formation of β-C_2S. The limestone begins to decarbonate between 600°C and 900°C (for instance, $CaCO_3 \rightarrow CaO + CO_2$). The rate and temperature of decomposition depend not only on the temperature and pressure but also on the SiO_2 content in the limestone. After 1200°C and up to 1300°C, some of the constituents begin to melt. Finally, concrete exists in molten form between 1300°C and 1400°C. The liquefaction of concrete appears to initiate with the melting of the hardened cement paste followed by the aggregates, which have different melting points. Basalt exists at the lower limit of rock types at 1060°C, while quartzite does not melt under 1700°C [11].

2. Research method

2.1. Mix preparing and specimen curing

Twelve cubic 100*100mm specimens were prepared according to the BS1881 standard [12] to determine the compressive strength. Moreover, 12 cylindrical specimens were prepared according to ASTM C597 and ASTM C496 to determine the tensile strength [13,14]. To this end, 12 mix designs with 0, 10, and 20 wt% lightweight concrete and 0, 0.1, 0.4, and 0.8 wt% polypropylene (PP) fibers were prepared. The tests were designed to determine the mechanical properties of lightweight concrete containing MK and PP fibers at high temperatures. The amount of Leca was considered constant in all the mix designs. Each mix specimen was exposed to four different temperatures.

Moreover, all the specimens were covered with a plastic cover for 24 hours before the tests. On the test day, the concrete specimens were removed from water and dried for 24 hours at room temperature to determine the mechanical properties. During the tests, the specimens were maintained at 200°C, 400°C, and 600°C under stable conditions for one hour. The details of the mix designs are shown in Table 4 [15].

Table 1. Mix proportion (one cubic meter) [15]

Mix ID	Cement	Metakaolin		Water	W/C	Gravel	Leca	Sand	Limestone powder	Superplasticizer	PP fibers	
	kg	kg	%	kg		kg	kg	kg	kg	%	kg	%
P0M0	450	0	0	228	0.5	228.3	300	186.8	180	1.05	0	0
P0.1M0	450	0	0	228	0.5	215.4	300	181.4	180	1.14	1.8	0.1
P0.4M0	450	0	0	228	0.5	221.7	300	160	180	1.1	3.6	0.4
P0.8M0	450	0	0	228	0.5	228.3	300	163	180	1.72	7.2	0.8
P0M10	405	45	10	228	0.5	221.7	300	171	180	1.23	0	0
P0.1M10	405	45	10	228	0.5	228.3	300	181.4	180	1.23	1.8	0.1
P0.4M10	405	45	10	228	0.5	215.4	300	176.2	180	1.26	3.6	0.4
P0.8M10	405	45	10	228	0.5	221.7	300	163	180	1.23	7.2	0.8
P0M20	360	90	20	228	0.5	215.4	300	186.8	180	1.42	0	0

P0.1M20	360	90	20	228	0.5	221.7	300	165.8	180	1.38	1.8	0.1
P0.4M20	360	90	20	228	0.5	228.3	300	176.2	180	1.7	3.6	0.4
P0.8M20	360	90	20	228	0.5	215.4	300	163	180	1.42	7.2	0.8

Based on BS1881, the lightweight concrete specimens were subjected to compressive strength tests at 20°C, 200°C, 400°C, and 600°C. The compressive strengths of the mixes with different MK percentages can be observed in the figure. Tables 2 and 3 display the compressive and tensile strength results of lightweight concrete with different percentages of PP fibers and MK at various temperatures. As can be seen, the 28-day compressive strength of lightweight concrete reduced gradually with a rise in temperature.

Table 2. Compressive strength test results [15]

Mix ID	Compressive strength (MPa)			
	20 °C	200 °C	400 °C	600 °C
P0M0	14.27	16.22	15.12	10.88
P0.1M0	15.12	15.96	15.34	9.31
P0.4M0	17.19	18.18	16.52	9.86
P0.8M0	19.86	18.17	16.2	10.27
P0M10	17.2	18.08	18.02	11.86
P0.1M10	18.05	19.16	18.09	10.84
P0.4M10	19.16	18.18	16.56	11.74
P0.8M10	20.14	19.07	16.19	11.65
P0M20	16.79	17.77	16.7	10.61
P0.1M20	17.06	18.18	16.59	10.57
P0.4M20	18.07	17.2	15.99	10.51
P0.8M20	19.17	18.88	15.12	10.39

Table 3.Tensile strength results of the specimens at different temperatures [15]

Mix ID	Tensile strength (MPa)			
	20 °C	200 °C	400 °C	600 °C
P0M0	1.22	1.18	1.04	0.97
P0.1M0	1.44	1.27	1.11	1.02
P0.4M0	1.73	1.29	1.23	1.15
P0.8M0	2.1	1.82	1.7	1.25
P0M10	1.56	1.4	1.2	0.9
P0.1M10	1.7	1.52	1.4	0.94
P0.4M10	1.91	1.78	1.45	1.05
P0.8M10	2.29	2.18	1.83	1.67
P0M20	1.67	1.56	1.3	0.8
P0.1M20	1.73	1.62	1.34	0.89

P0.4M20	1.91	1.76	1.41	0.94
P0.8M20	2.36	2.31	1.93	1.36

2.2. Artificial Neural Network (ANN)

ANN is a data processing system inspired by the human brain. In this system, data is processed in small processors interconnected in a network and functioning in parallel to solve a problem. ANN is the basis of artificial intelligence, which seeks to simulate the human brain in order to solve problems deemed difficult or impossible by human or statistical standards. These networks possess self-learning capabilities, which enable them to achieve better results with increased data input.

They consist of processing units with inputs and outputs. The inputs are what the ANN learns from in order to produce the desired output.

ANNs are structured similarly to the human brain with nerve nodes interconnected in a web. The human brain is composed of billions of cells called neurons. Each neuron consists of a cell tasked with processing information.

ANNs contain hundreds or thousands of artificial neurons, or processors, connected via synapses. The processors consist of inputs and outputs. The inputs receive various forms of data, and the neural network attempts to learn the information in order to produce outputs.

ANNs are employed for modeling nonlinear problems. They give the inputs to mathematical functions and present outputs, which are usually accompanied by some error. This error can be reduced by modifying the weights of inputs via feedback.

ANN resembles the brain in two ways:

* It acquires knowledge from its surrounding via a learning process.
* Weighting the interneuron connections occurs similarly to that in the information storage system in the human brain.

2.3. Model description and training

2.3.1. Dataset

Obtaining an ANN capable of correctly predicting results requires accurate and sufficient data from influential parameters. For this reason, 12 specimens with varying mix designs were prepared and tested in the laboratory. Different percentages of cement, MK, gravel, sand, superplasticizer, and PP fibers along with temperature were considered the 7 inputs of the ANN, and the compressive and tensile strengths were considered the 2 outputs (Tables 1, 2, and 3).

2.3.2. Optimal ANN structure

The performance of an ANN depends on its structure and parameter adjustments. One of the most important issues in ANNs is finding the optimal structure by determining the optimal number of layers and the optimal number of neurons in the hidden layer via trial and error. The trial and error method is valid in this regard since no definite rule has been introduced for determining the optimal structure of ANNs and adjusting the parameters.

The stop criterion for training is the mean square error (MSE), which represents the mean square of the difference between the model prediction (network output) and the actual (target) value. Lower MSE values reflect better performance of the network, with a value of zero representing error-free performance.

$$MSE = \frac{1}{n}\sum_{i=1}^{n}(y_i - \hat{y}_i)^2 \quad (1)$$

n = the number of predicted values

y_i = the true value of the i-th datum

$\hat{y}_i$ = the predicted value of the i-th datum

The regression values (R-values) express the strength of the relationship between the output and the target values. In fact, they measure the correlation between these two variables. The R-values always lie within the range (-1,1). The closer the correlation coefficient to 1, the stronger the correlation.

$$R = \sqrt{1 - \frac{\sum (y - \hat{y})^2}{\sum \hat{y}^2}} \tag{2}$$

where y denote the true values, and $\hat{y}$ represent the predicted values. A regression value of 1 means close correlation, while a value of zero reflects a distant correlation between the network output and the target.

The ANN used in this study is an MLP and was trained with 7 inputs and 1 hidden layer with 5 neurons. 70% of the data were selected for training, 15% for validation, and the remaining 15% for testing (Fig. 1).

The Bayesian Regularization algorithm, called using the nftool command, was used to train the network and determine the coefficients. The data were normalized using the following formula and used to design the network.

$$Z = \frac{X - \min(x)}{\max(x) - \min(x)} \tag{3}$$

X= data from Tables 1, 2, and 3

Z= normalized values

Table 4 summarizes the ANN parameters used in this research.

Table 4. ANN parameters

Parameter name	Description
Neural network structure	MLP
Optimization function	Bayesian Regularization
Percentage of training data	70%
Percentage of validation data	15%
Percentage of testing data	15%

3. Results and discussion

The MSE and R-value criteria were considered the basis for selecting the optimal network. Through trial and error, MSE and R-values of 0.9916 and 0.00233 were obtained.

The obtained optimal network was able to accurately predict the compressive and tensile strengths for the datasets after training. Fig. 3 depicts the actual and predicted regressions for the training, validation, and testing datasets, indicating the validity of the network for this dataset.

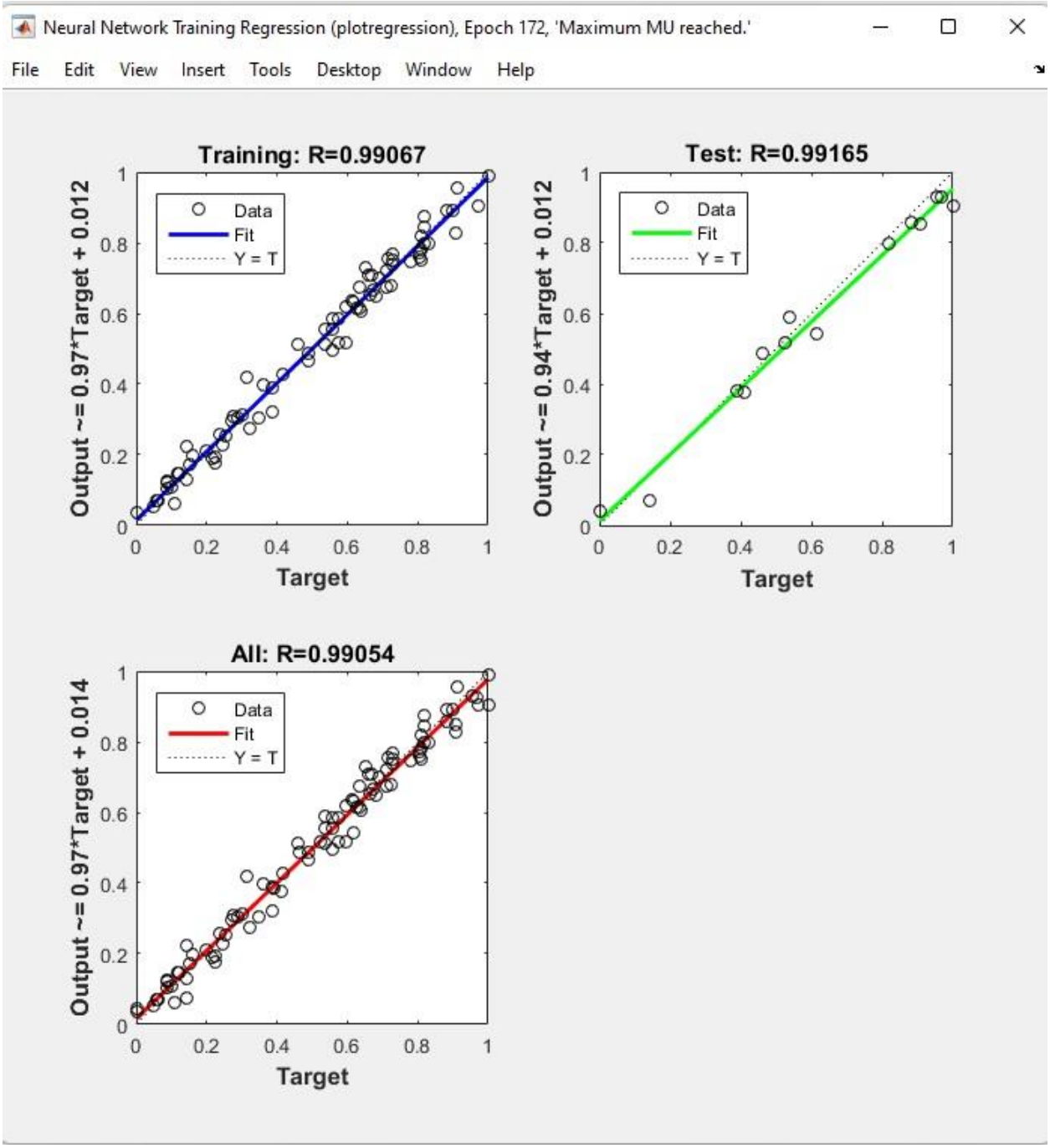

Figure 1. Actual versus predicted regressions for the training, validation, and testing datasets

The outputs estimated by the program were normalized. These values were decoded using Formula 1 for comparing them with the true values. Specifically, the Z-values from the program output were input to Formula 1, and the X values were obtained. A study of the errors between the true and values predicted by the ANN indicates that the maximum errors for compressive strength at temperatures of 20°C, 200°C, 400°C, and 600°C were 5.11, 3.46, 5.15, and 8.24, respectively

(Table 5). Moreover, zero error was obtained for the tensile strength (Table 6), which demonstrates the high accuracy of the designed ANN.

Table 5. MLP predictions

Predicted compressive strength (MPa)								
	20 °C		200 °C		400 °C		600 °C	
Mix ID	(MPa)	Error (%)	(MPa)	Error (%)	(MPa)	Error (%)	(MPa)	Error (%)
P0M0	14.27	-4.22	15.87	2.16	15.34	-1.42	10.68	1.85
P0.1M0	15.12	-3.69	16.23	-1.67	15.32	0.14	9.76	-4.78
P0.4M0	17.19	-1.63	17.96	1.23	16.37	0.90	9.89	-0.29
P0.8M0	19.86	3.76	18.80	-3.46	15.99	1.29	10.42	-1.43
P0M10	17.2	-0.71	18.22	-0.75	17.56	2.57	12.08	-1.88
P0.1M10	18.05	1.90	18.53	3.28	17.47	3.41	11.73	-8.24
P0.4M10	19.16	4.46	18.48	-1.64	16.99	-2.60	11.40	2.91
P0.8M10	20.14	5.11	18.98	0.46	16.64	-2.76	11.37	2.44
P0M20	16.79	-0.52	17.41	2.04	16.34	2.18	10.86	-2.40
P0.1M20	17.06	-2.54	17.96	1.20	16.53	0.37	10.86	-2.77
P0.4M20	18.07	1.58	17.62	-2.46	15.17	5.15	9.97	5.16
P0.8M20	19.17	-2.66	18.60	1.47	14.87	1.68	10.48	-0.84

Table 6. MLP predictions

Mix ID	Predicted tensile strength (MPa)							
	20 °C		200 °C		400 °C		600 °C	
	(MPa)	(%)	(MPa)	(%)	(MPa)	(%)	(MPa)	(%)
P0M0	1.22	0.00	1.18	0.00	1.04	0.00	0.97	0.00
P0.1M0	1.44	0.00	1.27	0.00	1.11	0.00	1.02	0.00
P0.4M0	1.73	0.00	1.29	0.00	1.23	0.00	1.15	0.00
P0.8M0	2.1	0.00	1.82	0.00	1.7	0.00	1.25	0.00
P0M10	1.56	0.00	1.4	0.00	1.2	0.00	0.9	0.00
P0.1M10	1.7	0.00	1.52	0.00	1.4	0.00	0.94	0.00
P0.4M10	1.91	0.00	1.78	0.00	1.45	0.00	1.05	0.00
P0.8M10	2.29	0.00	2.18	0.00	1.83	0.00	1.67	0.00
P0M20	1.67	0.00	1.56	0.00	1.3	0.00	0.8	0.00
P0.1M20	1.73	0.00	1.62	0.00	1.34	0.00	0.89	0.00
P0.4M20	1.91	0.00	1.76	0.00	1.41	0.00	0.94	0.00
P0.8M20	2.36	0.00	2.31	0.00	1.93	0.00	1.36	0.00

For further analysis, the true (Tables 2 and 3) and predicted (Tables 5 and 6) values were plotted in Fig. 4. According to this figure.

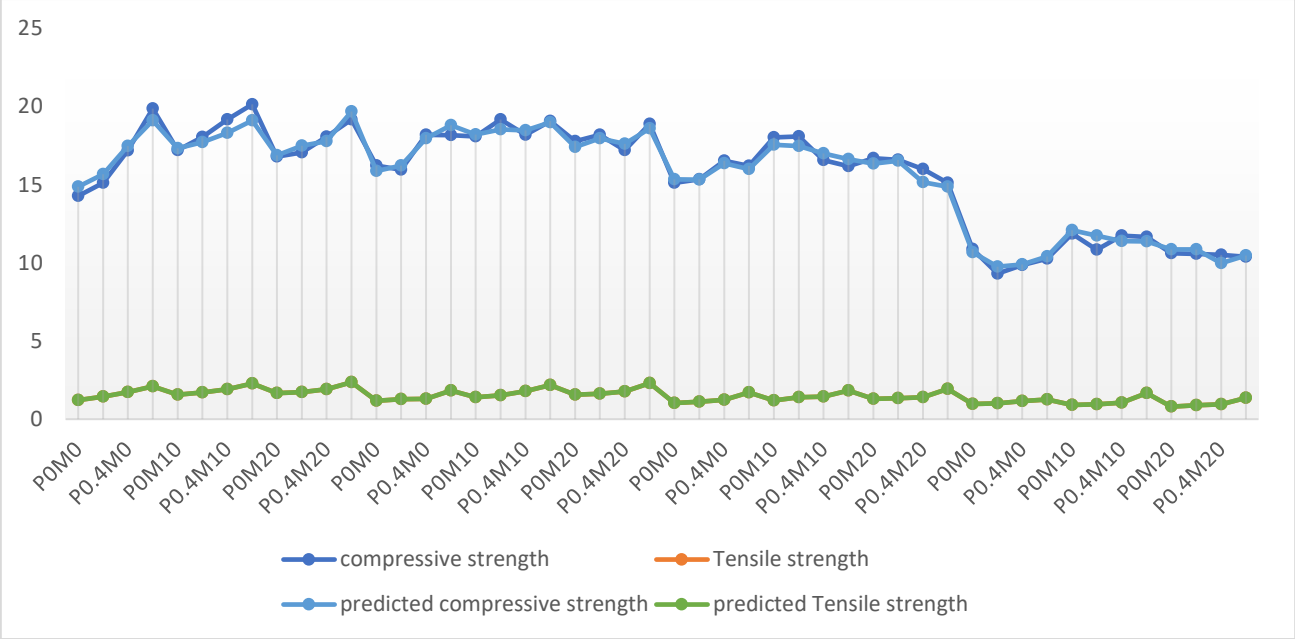

Figure 2. Comparison of experimental and numerical quantities

4. Conclusion

1. In this research, the ANN method was employed to estimate the mechanical properties of lightweight fiber-reinforced concrete containing MK.

2. The 7 input parameters of the network were the percentages of cement, MK, gravel, sand, superplasticizer, and PP fibers along with temperature, and the 2 outputs of the network were the compressive and tensile strengths. For this purpose, data for 12 concrete specimens were collected from [15], which is based on experimental studies.

3. A comparison between the values estimated by the ANN and the true values demonstrates the accuracy, efficiency, and reliability of the designed network.

4. The correlation coefficient was above 99% for the training, validation, and testing datasets. This indicates the effectiveness of the neural network in predicting the compressive and tensile strengths of the lightweight fiber-reinforced concrete containing Mk.

5. The maximum errors for the compressive strength data at temperatures of 20, 200, 400, and 600 were 5.11%, 3.46%, 5.15%, and 8.24%, respectively, while an error of 0 was obtained for the tensile strength at all temperatures.

6. Based on the results, one may conclude that the designed neural network can be used to accurately predict the compressive and, especially, tensile strengths of lightweight fiber-reinforced concrete containing MK.

References

1. Ahmad, A., Ostrowski, K.A., Maślak, M., Farooq, F., Mehmood, I., Nafees, A. Comparative Study of Supervised Machine Learning Algorithms for Predicting the Compressive Strength of Concrete at High Temperature. Materials. 2021. 14(15). DOI:10.3390/ma14154222. URL: https://www.mdpi.com/1996-1944/14/15/4222.
2. Bayat, M., Delnavaz, A. Determination of Lateral load Capacity of Steel Shear Walls Based on Artificial Neural Network Models. Journal of Structural Engineering and Geo-Techniques. 2020. 10(1). Pp. 35–43. URL: https://jseg.qazvin.iau.ir/article_665835.html.

3. Tufail, M., Shahzada, K., Gencturk, B., Wei, J. Effect of Elevated Temperature on Mechanical Properties of Limestone, Quartzite and Granite Concrete. International Journal of Concrete Structures and Materials. 2017. 11(1). Pp. 17–28. DOI:10.1007/s40069-016-0175-2. URL: https://doi.org/10.1007/s40069-016-0175-2.
4. Poon, C.-S., Azhar, S., Anson, M., Wong, Y.-L. Performance of metakaolin concrete at elevated temperatures. Cement and Concrete Composites. 2003. 25(1). Pp. 83–89. DOI:https://doi.org/10.1016/S0958-9465(01)00061-0 URL: https://www.sciencedirect.com/science/article/pii/S0958946501000610.
5. Demirel, B., Gultekin, E., Alyamac, K.E. Performance of Structural Lightweight Concrete containing Metakaolin after Elevated Temperature. KSCE Journal of Civil Engineering. 2019. 23(7). Pp. 2997–3004. DOI:10.1007/s12205-019-1192-x. URL: https://doi.org/10.1007/s12205-019-1192-x.
6. Nadeem, A., Memon, S.A., Lo, T.Y. The performance of Fly ash and Metakaolin concrete at elevated temperatures. Construction and Building Materials. 2014. 62. Pp. 67–76. DOI:https://doi.org/10.1016/j.conbuildmat.2014.02.073. URL: https://www.sciencedirect.com/science/article/pii/S0950061814002360.
7. Mehdipour, S., Nikbin, I.M., Dezhampanah, S., Mohebbi, R., Moghadam, H., Charkhtab, S., Moradi, A. Mechanical properties, durability and environmental evaluation of rubberized concrete incorporating steel fiber and metakaolin at elevated temperatures. Journal of Cleaner Production. 2020. 254. Pp. 120126. DOI: https://doi.org/10.1016/j.jclepro.2020.120126. URL: https://www.sciencedirect.com/science/article/pii/S0959652620301736.
8. Albidah, A., Alqarni, A.S., Abbas, H., Almusallam, T., Al-Salloum, Y. Behavior of Metakaolin-Based geopolymer concrete at ambient and elevated temperatures. Construction and Building Materials. 2022. 317. Pp. 125910. DOI:https://doi.org/10.1016/j.conbuildmat.2021.125910. URL: https://www.sciencedirect.com/science/article/pii/S0950061821036436.
9. Ofuyatan, O.M., Agbawhe, O.B., Omole, D.O., Igwegbe, C.A., Ighalo, J.O. RSM and ANN modelling of the mechanical properties of self-compacting concrete with silica fume and plastic waste as partial constituent replacement. Cleaner Materials. 2022. 4. Pp. 100065. DOI: https://doi.org/10.1016/j.clema.2022.100065. URL: https://www.sciencedirect.com/science/article/pii/S2772397622000259.
10. Harmathy, T.Z., Berndt, J.E. Hydrated portland cement and lightweight concrete at elevated temperatures. Research Paper (National Research Council of Canada. Division of Building Research); no. DBR-RP-280. 1966. DOI:10.4224/40001488.
11. Naus, D., others. The effect of elevated temperature on concrete materials and structures: a literature review. Division of Engineering Technology, Office of Nuclear Regulatory Research~…, 2006.

[12] BS1881, Method for determination of compressive strength of concrete cubes. British Standard Institution.

[13] ASTM C597. Standard test method for pulse velocity through concrete. 2016.

[14] ASTM C496. Standard test method for splitting tensile strength of cylindrical concrete specimens. Annual book of ASTM standards; 2008.

15. Balgourinejad, N., Haghighifar, M., Madandoust, R., Charkhtab, S. Experimental study on mechanical properties, microstructural of lightweight concrete incorporating polypropylene fibers and metakaolin at high temperatures. Journal of Materials Research and Technology. 2022. 18. Pp. 5238–5256. DOI:https://doi.org/10.1016/j.jmrt.2022.04.005. URL: https://www.sciencedirect.com/science/article/pii/S2238785422005051.